Observability Function of the BRAMS network

Hervé Lamy[1], Cis Verbeeck[2], Joachim Balis[1], Michel Anciaux[1], Stijn Calders[1], Antoine Calegaro[1], and Antonio Martínez Picar[2]

[1] **Royal Belgian Institute for Space Aeronomy, Avenue Circulaire 3, 1180, Brussels, Belgium**
herve.lamy@aeronomie.be

[2] **Royal Observatory of Belgium, Brussels, Belgium**
cis.verbeeck@oma.be

For meteor showers, the observed activity based on the raw counts of meteor echoes recorded by a radio forward scatter system is modulated by the position of the radiant throughout the day and does not truly reflect the real activity of the shower. A possibility to correct these raw counts is to compute the so-called Observability Function (OF) which contains a geometrical part and a sensitivity part. In this paper, we remind the most important characteristics of the OF described in Verbeeck (1997) and discuss them in the context of the BRAMS forward scatter network. We conclude with future works on how to apply the OF to the raw counts of a few main meteor showers obtained from the Citizen Science project, the Radio Meteor Zoo.

1 Introduction

When a meteoroid enters Earth's atmosphere, it creates an ionized trail along its path with an electron density which is locally much higher than the ambient ionosphere. This trail can temporarily reflect radio waves transmitted from the ground and be detected by a receiver tuned to the same frequency. The reflected signal is usually called a meteor echo. In a forward scatter system, the transmitter and the receiver are not co-located (see Figure 1).

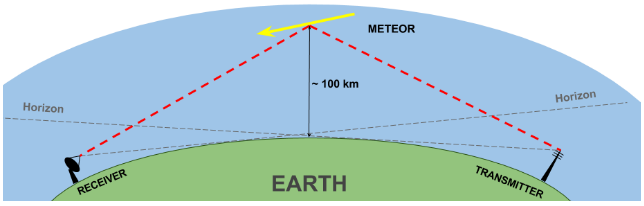

Figure 1 – Geometry of a forward scatter set-up.

This reflection is specular, which means that most of the reflected power comes from a small region along the meteoroid trajectory centered on the specular reflection point, whose position depends on the locations of the transmitter and the receiver, and on the meteoroid path itself (see Figure 2).

This reflection point is tangential to a prolate ellipsoid having the transmitter and the receiver as the two foci (Wislez et al. 2006, Lamy et al. 2016). This puts important geometrical constraints on whether a specific meteoroid trajectory can be detected or not by a given receiving station since the position of the reflection point must fall within the so-called meteor zone. This zone is roughly delimited in altitude between 85 km (below which most of the meteoroids have been fully ablated) and 110 km (above which the density of the atmosphere is too scarce to produce sufficient ionization

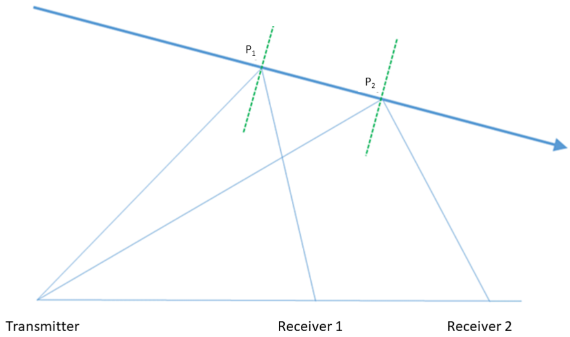

Figure 2 – Specularity of the forward scatter radio wave reflection. The positions of the reflection points on the meteoroid path (in blue) are different for receivers 1 and 2.

and a strong enough reflected signal which can be detected at the ground).
As a consequence, for meteor showers, the observed activity based on the raw counts of meteor echoes recorded by a receiving station is modulated by the position of the radiant throughout the day and does not truly reflect the real activity of the shower. A possibility to correct these raw counts is to compute the so-called Observability Function (OF) introduced by Hines (1958) and further developed by Verbeeck (1997). This OF contains a geometrical part which provides the location of all potentially observable meteor trails at a given moment for the considered radiant and transmitter and receiver locations, and another part which takes into account which fraction of these trails will actually be detected by the receiving station. Indeed, whether a meteor echo will be detected at the station also depends on the sensitivity of the receiving chain, on the power transmitted and on the ionization at the reflection point, the latter depending on the initial mass of the meteoroid.
In this paper, we remind the most important aspects of how to compute the OF, as described in detail in Verbeeck (1997), and provide results for one receiv-

ing station of the BRAMS[1] network to emphasize the importance of the geometry. We also describe how we take into account important characteristics of the BRAMS system to determine the sensitivity of the receiving chain such as the gains of the transmitting and receiving antennas in the directions of the meteor echoes. Finally, we discuss our objectives to apply the OF to the raw counts of a few meteor showers obtained from outputs of the Citizen Science project, the Radio Meteor Zoo (e.g. Calders et al. 2018), which has been developed since 2016 in cooperation with Zooniverse [2].

2 The BRAMS network

The BRAMS (Belgian RAdio Meteor Stations) network is a Belgian project using forward scatter of radio waves to detect and characterize meteoroids. It comprises a dedicated transmitter located in the South-West of Belgium and 44 receiving stations spread all over the Belgian territory and neighbouring countries (see Figure 3 for status in October 2022).

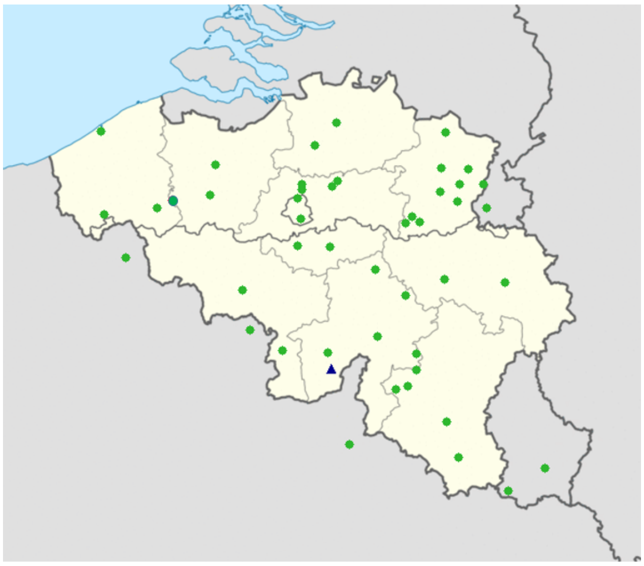

Figure 3 – Map of the BRAMS network in October 2022. The blue triangle is the transmitter located in Dourbes while the green dots are the 44 active receiving stations at the time.

The transmitter emits a right-handed circularly polarized continuous radio wave with no modulation at a frequency of 49.97 MHz with a power of 130 Watts. The transmitter is made of a crossed dipole with a metallic grid of 8×8 meters acting as the reflector to transmit more power towards zenith. All the receiving stations are using a 3-element Yagi antenna set-up vertically and oriented in azimuth towards the transmitter. In October 2022, approximately one third of the receiving stations were using analog ICOM-R75 receivers, an external sound card to sample the signal coming from the antenna, and were controlled by the freeware program Spectrum Lab running on a PC (see e.g. Lamy et al. 2015). The other two-third uses digital SDR-RSP2 receivers controlled by a Linux system running on a Raspberry Pi (Anciaux et al. 2020). All stations are equipped with a Garmin GPS that provides timestamps to the BRAMS data and allows a time synchronization between the receiving stations. Additional features of the receiving stations are not described here and we refer the reader to previous publications in the Proceedings of the IMC.

[1] https://brams.aeronomie.be
[2] https://www.radiometeorzoo.be

3 Observability Function: geometrical part

For a given position of the radiant at a given time, all trajectories from meteoroids belonging to the meteor shower are parallel. As described above, not all of them can be detected by a given pair Transmitter-Receiver since the altitude of their reflection point might not be adequate. The first step to compute the OF at a given time is to calculate the positions of all possible reflection points. As shown in Verbeeck (1997), the specularity condition leads to a simple property

$$\cos \rho + \cos \tau = 0 \tag{1}$$

where τ and ρ are the angles made between the meteoroid trail and the directions between respectively the transmitter / the receiver and the specular reflection point (see Figure 4).

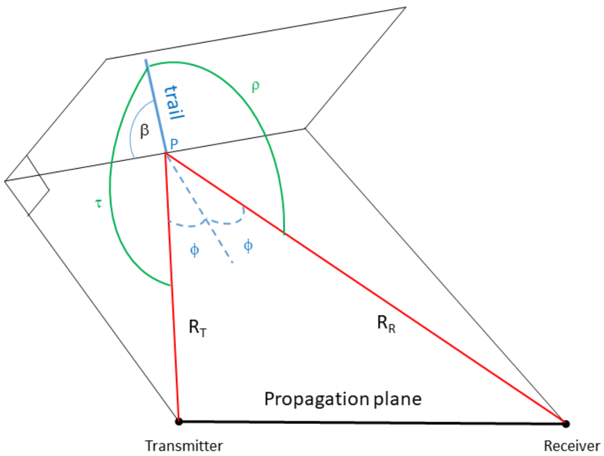

Figure 4 – Geometry of the radio forward scatter. The radio wave (in red) propagates from the transmitter to the reflection point P on the meteoroid path and down to the transmitter. The meteor trail (in blue) is inclined by an angle β to the propagation plane. The perpendicular to the meteor trail (dashed blue line) at the specular reflection point P divides the scattering angle in two equal parts ϕ. τ and ρ (in green) are the angles made between the meteor trail and directions from the transmitter/receiver to the reflection point P.

Equation 1 depends on the Cartesian coordinates of the specular point P ($= x_0$, y_0, z_0), of the direction cosines of the radiant ($= l$, m, n), and of the distances R_T and

R_R. The direction cosines are linked to the traditional elevation θ and azimuth ϕ via

$$l = \sin\theta\,\cos\phi \tag{2}$$
$$m = \sin\theta\,\sin\phi \tag{3}$$
$$n = \cos\theta \tag{4}$$

It can be shown that at a fixed altitude z_0, this equation leads to a 6^{th} order polynomial in x_0, y_0. Solving this polynomial provides curves which are the loci of the potential reflection points for this meteor shower at a given time and a given altitude. Figure 5 is an example of curves obtained for the pair Dourbes (transmitter) - Humain (receiver) separated by a distance of $\sim$ 50 km. Three different altitudes z_0 = 90, 100 and 110 km are shown, which illustrates that the variation of the curves with altitude are rather smooth.

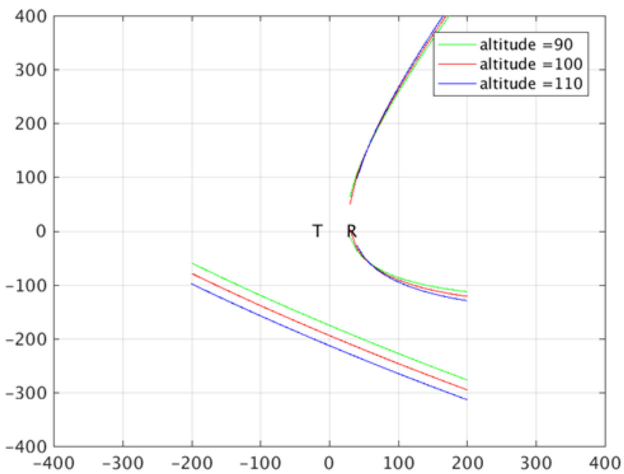

Figure 5 – Location of potential specular reflection points in the horizontal plane at 3 different altitudes (90, 100 and 110 km) for a distance of 50 km between the transmitter T and the receiver R and for a radiant located at an elevation $\theta = 30°$ and an azimuth $\phi = 60°$. The reference frame is centered on the point at half-distance between T and R and the x-axis is oriented along the T-R line.

To obtain a three-dimensional surface, an integration must be done in altitude between the various curves. This is now done numerically and does not require anymore the use of the assumptions described in Verbeeck (1997). Since the variation of the curves at different altitudes is rather smooth, the integration is done with curves separated by 5 km to save some computational time. It was checked that decreasing this altitude bin does not deteriorate the results significantly.

4 Observability function: the sensitivity part

Now that the geographical location of all specular reflection points has been found, we need to determine what will be the minimum electron density at each potential reflection point to produce a signal that can be detected at the receiver. For that we rely on the formula giving the power of an underdense meteor echo, which is an extension of the formula valid for a back scatter system (radar) and taking into account the more complex geometry of a forward scatter system (Mc Kinley 1961, Wislez et al. 2006) :

$$P_u(r_0 = 0) = \frac{P_T\,G_T\,G_R\,\lambda^3\,r_e^2\,\alpha^2\,\sin^2\gamma}{16\,\pi^2\,R_T\,R_R\,(R_T + R_R)\,(1 - \sin^2\phi\,cos^2\beta)} \tag{5}$$

$$P_{u,max} = P_u(r_0 = 0)\,\times\,\exp\left(\frac{-8\,\pi^2\,r_0^2}{\lambda^2\,\sec^2\phi}\right) \tag{6}$$

$$P_u(t) = P_{u,max} \times \exp\left(\frac{-32\,\pi^2\,D\,t}{\lambda^2\,\sec^2\phi}\right) \tag{7}$$

Equation (5) is the formula for underdense meteor assuming all electrons in the trail lie on an infinitely thin line along the meteoroid path. A much better assumption is to consider that the electrons are located on a cylinder with initial radius r_0 and this is taken into account in equation (6). We see that for very small initial radii, if $r_0 \ll \lambda$, the approximation of equation (5) stands. Equation (7) describes the time evolution of the ionized meteor trail when the dominant mechanism is the ambipolar diffusion of the electrons in the surrounding neutral atmosphere. Note that the Fresnel oscillations are not taken into account here. A typical underdense meteor echo is therefore composed of a sharp rise (a few ms of duration) to a maximum given by Equation (6) followed by an exponential decay. An example is shown in Figure 6.

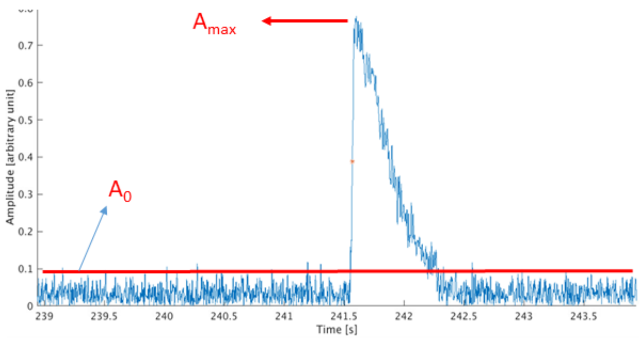

Figure 6 – Example of an underdense meteor echo observed by the BRAMS network. The envelope of the amplitude of the signal is shown in arbitrary units. The power of the signal is the square of this quantity. A_0 is an estimate of the noise level in the data while A_{max} is the peak value of the meteor echo.

In equation (5), the numerator contains several “technical” parameters, linked to the charateristics of the transmitter and the receiver. λ is the wavelength ($\sim$ 6m in the case of BRAMS), P_T is the transmitted power, G_T and G_R are respectively the gains of the transmitting and receiving antennas and depend on the direction of arrival of the signal. All these parameters can be monitored regularly and accurately. $\sin^2\gamma$ is related to the polarization of the signal (the transmitted signal with BRAMS is circularly polarized). r_e is the classical Bohr radius. The denominator in equation (5) contains only parameters related to the geometry (see Figure 4). Hence for each point on the surface calculated in section 3, these parameters are known.

For the BRAMS network, so far the transmitted power P_T has been measured first using a wattmeter and a dummy load at the exit of the power amplifier, then taking into account losses in the coaxial cables going to the antennas. The dummy load cannot stand a high power for a long time and the wattmeter is analog. As a consequence we estimate that the accuracy on the transmitted power ($\sim$ 130W) is of the order of $\sim$ 10%. We are currently procuring additional material in order to regularly measure the power at the exit of the amplifier with a higher accuracy (typically a few %). For the gain of the transmitting antenna G_T, we have designed a payload suspended below an Helium-filled balloon and two short perpendicular dipole antennas located just below it, that we use to sample the far-field of the antenna at roughly 10 m height above the antenna in an horizontal plane (see Figure 7). The payload contains two receivers connected to the two dipoles and a magnetometer, inclinometer, a GPS and a webcam to allow us to calculate accurately the position and attitude of the payload. The transmitter emits at a very small part of the nominal power to avoid saturating the receivers. Results provide G_T as a function of azimuth and elevation and will be published elsewhere.

The same kind of experiment cannot be done to measure the gain of the receiving antennas G_T for practical reasons and for lack of time. Therefore, for the receiving antennas we rely on the theoretical pattern of a 3-elements Yagi antenna set up vertically or on electromagnetic simulations such as the ones carried out by Martínez Picar et al (2015). The real pattern is close to the theoretical one because when the antenna is set up vertically, the reflector (lowest element in Figure 8) is protecting well e.g. from modifications of the conductive properties of the ground.

The remaining parameter missing in Equation (5) is the angle γ which is the angle between the electric field vector of the transmitted radio wave and the direction to the receiver. Its computation was derived for horizontal polarization of the transmitted signal in Suleymanova et al (2007). This calculation is currently being adapted to the BRAMS network to take into account the circular polarization of the transmitted signal. In Equation (6), there is an additional parameter: the initial trail radius r_0 which is difficult to measure and is usually estimated using experimental or empirical relations such as e.g. (Suleymanova, 2007) :

$$r_0 = 1.65\sqrt{\frac{v}{40}}\exp\left(\frac{z_0 - 95}{2H}\right) \tag{8}$$

where r_0 is expressed in meters, v is the speed of the meteoroid (in km/s) and H is the atmospheric scale height (in km).

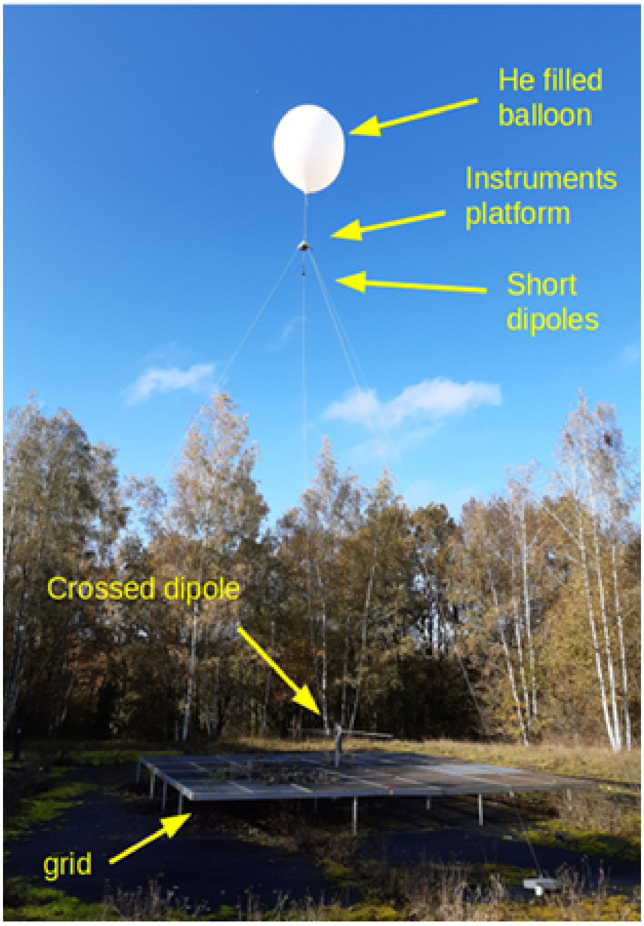

Figure 7 – Picture of the experiment conducted with a payload, two short dipoles and an Helium-filled balloon to measure the gain G_T of the transmitting antenna of BRAMS. See text for details.

Figure 8 – Receiving antenna at the BRAMS station located in Uccle. It is a 3-elements Yagi antenna set up vertically.

With all these parameters and equations in hand, we can then write Equation (6) as

$$P_{u,max} = K \times \alpha^2 \tag{9}$$

or alternatively

$$A_{u,max} = \sqrt{K} \times \alpha \tag{10}$$

where K can be determined for a given station and all points computed on the surface of potential reflection points. α is the electron line density (in m^{-1}). For a meteor echo to be detectable, the peak value $A_{u,max}$ must be larger than the level of noise A_0, recorded locally at the station and at that particular time (see Figure 6). A_0 is computed directly from the BRAMS data. This puts a constraint for a minimum value of α which turns into a minimum value for the mass m of the incoming meteoroid since $\alpha \sim m \cos Z$ where Z is the zenithal angle of the meteoroid path.

The mass distribution of meteoroids from a meteor shower is usually characterized by a power law with an exponent called the mass index s :

$$N(m) \propto m^{1-s} \tag{11}$$

$N(m)$ is the cumulative number of objects with a mass larger than m. s can be obtained either from previous measurements or it can be obtained from the cumulative distribution of amplitude of radio meteor echoes (e.g. Blaauw et al, 2011). With this value of s, the probability that $A_{u,max} > A_0$ can be calculated (see Verbeeck 1997 for mathematical details).

5 Summary and perspectives

The Observability Function is a tool to convert the observed activity of a meteor shower to a more realistic activity, taking into account the specularity condition of the radio wave reflections and the particular sensitivity of the transmitter-receiver pair. This tool was developed by Verbeeck (1997) and has been extended recently to better take into account the integration over altitude of the location of the specular reflection points. This replaces assumptions made in this paper due to the limited computing facilities at the time. We have started developing this tool for the specific case of the BRAMS forward scatter network, measuring or computing gains of the transmitting and receiving antennas, calculating the specific surface containing the reflection points for a specific receiving station, taking into account the circular polarization of the transmitted wave, etc. This work is still in progress.

The goal is eventually to be able to calculate the OF for a given meteor shower at a given time and a given receiving station of the BRAMS network. The result can be presented as a polar plot showing the OF as a function of azimuth and elevation of the radiant, as was done by Zigo (2008) for the Lecce-Modra system.

With the Radio Meteor Zoo citizen science project, we have been able to obtain the observed activity of several meteor showers at two different receiving stations of the BRAMS network (namely Oudsbergen and Humain). These stations are not located at the same distance to the transmitter, they have different sensitivities, and slightly different geometries. Hence, we aim to compute their OF for each hour and correct their observed activities of the meteor shower. In principle we should then find "corrected" activities that are consistent with each other, proving that the OF works.

There are of course a number of limitations with this approach. The main one is probably that the sensitivity part of the OF (described in section 4) assumes underdense meteor echoes while a non-negligible part of meteor echoes observed by the BRAMS network during meteor showers are intermediate or overdense. Equations (5) and (6) might therefore not be appropriate anymore. Other equations might be used instead such as those developed by Pecina (2016) for a radar (back scatter) system. An extension to the forward scatter case would then be needed.

Acknowledgements

The BRAMS network is funded partly by the Solar-Terrestrial Center of Excellence[3]. The BRAMS project is an active Pro-Am collaboration. We would like to thank all operators hosting the receiving stations.

References

Anciaux, M. L. H. M. P. A. R. S. C. S. C. A. and Verbeeck C. (2019). "The brams receiving station v2.0". In Pajer, U. R. J. G. M. and Verbeeck C., editors, *Proceedings of the International Meteor Conference,* Bollmansruh, Germany, 2019. IMO, pages 39–42.

Blaauw, R.C. ; Campbell-Brown M. and Weryk R. (2011). "A meteoroid stream survey using the canadian meteor orbit radar - iii. mass distribution indices of six major meteor showers". *MNRAS*, **413**, 3322–3329.

Calders, S. L. H.-M. P. A. T. C. V. C. and Gamby E. (2018). "The radio meteor zoo: Involving citizen scientists in radio meteor research". In Gyssens M. and Rault J.-L., editors, *Proceedings of the International Meteor Conference,* Petnica, Serbia, 2017. IMO, pages 13–15.

Hines C. (1958). "Diurnal variations in the number of shower meteors detected by the forward-scattering of radio waves. part iii. elipsoidal theory". *Canadian Journal of Physics*, **36**, 117–126.

Lamy H. and Tétard C. (2016). "Retrieving meteoroids trajectories using brams data : preliminary simulations". In Roggemans A. and Roggemans P., editors, *Proceedings of the International Meteor Conference,* Egmond, The Netherlands, 2016. IMO, pages 143–147.

Lamy, H. ; Anciaux M. R. S. . C. S. . G. E. . M. P. A. . and Verbeeck C. (2015). "Recent advances in the brams network". In Rault J.-L. and Roggemans

[3]https://www.stce.be/

P., editors, *Proceedings of the International Meteor Conference,* Mistelbach, Austria, 2015. IMO, pages 171–176.

Martínez Picar, A. ; Marqué C. . A. M. and Lamy H. (2015). "Directional pattern measurement of the brams beacon antenna system". In Rault J.-L. and Roggemans P., editors, *Proceedings of the International Meteor Conference,* Mistelbach, Austria, 2015. IMO, pages 177–179.

McKinley D., editor (1961). *Meteor science and engineering.* McGraw-Hill,New York, USA.

Pecina P. (2016). "An analytical theory of radio-wave scattering from meteoric ionization - i. basic equation". *MNRAS*, **455**, 2200–2206.

Suleymanova S. (2007). "Calculating the meteoroid flux density of a meteor shower from radio forward scatter observations". In Bettonvil F. and Kac J., editors, *Proceedings of the International Meteor Conference,* Roden, The Netherlands, 2006. IMO, pages 162–174.

Verbeeck C. (1997). "Calculating the sensitivity of a forward scatter setup for underdense shower meteors". In Gyssens M. and Roggemans P., editors, *Proceedings of the International Meteor Conference,* Apeldoorn, The Netherlands, 1996. IMO, pages 122–132.

Wislez J.-M. (2006). "Meteor astronomy using a forward scatter set-up". In Verbeeck C. and Wislez J.-M., editors, *Proceedings of the International Meteor Conference,* Oostmalle, Belgium, 2005. IMO, pages 85–107.

Zigo P. (2008). "Observability function of the bologna - modra forward scatter system". *Contributions of the Astronomical Observatory Skalnaté Pleso*, **38**, 61–69.